Arabian Journal of Chemistry (2016) **9**, S1457–S1463

King Saud University

Arabian Journal of Chemistry

www.ksu.edu.sa
www.sciencedirect.com

ORIGINAL ARTICLE

Simultaneous intercalation and release of 2,4-dichloro- and 4-chloro-phenoxy acetates into Zn/Al layered double hydroxide

Abbas Matrod Bashi [a,b,*], **Mohd Zobir Hussein** [b,c], **Zulkarnain Zainal** [b,c], **Mawardi Rahmani** [c], **Didier Tichit** [d]

[a] *Faculty of Applied Medical Science, University of Karbala, 96432 Karbala, Iraq*
[b] *Advanced Materials and Nanotechnology Laboratory, Institute of Advanced Technology (ITMA), Malaysia*
[c] *Department of Chemistry, Faculty of Science, Universiti Putra Malaysia, 43400 UPM Serdang, Selangor, Malaysia*
[d] *Institut Charles Gerhardt UMR 5253 CNRS/UM2/ENSCM/UM1, Matériaux Avancés pour la Catalyse et la Santé, 8 rue Ecole Normale, 34296 Montpellier Cedex 5, France*

Received 3 August 2011; accepted 17 March 2012
Available online 29 March 2012

KEYWORDS

Layered double hydroxide;
2,4-Dichlorophenoxy acetic acid;
4-Chlorophenoxy acetic acid;
Controlled release;

Abstract A new nanohybrid compound was formed by the concurrent insertion of 2,4-dichlorophenoxy acetate (DPA) used as herbicides and 4-chlorophenoxy acetate (CPA) as plant growth regulator, the two guest anions into the interlamellar space of the host Zn/Al layered double hydroxide (LDH) using co-precipitation or spontaneous self-assembly method. Two different basal spacings of 2.54 and 1.97 nm were detected by PXRD of the nanohybrid accounting for the presence of two distinct intercalated phases. Direct insertion mass spectroscopy (DIMS) analyses confirm that both

---

Abbreviations: DPA, 2,4-dichlorophenoxy acetate; CPA, 4-chlorophenoxy acetate; LDH, Zn/Al layered double hydroxide; PXRD, X-ray diffractions; DIMS, direct insertion mass spectroscopy. The hybrids intercalated with DPA, CPA and with mixed biphase DPA and CPA were designated as DPA-Zn/Al, CPA-Zn/Al and DCPA-Zn/Al, respectively; FTIR, fourier transform infrared; TGA/DTG, thermal gravimetric and differential thermal gravimetric analysis.

[*] Corresponding author. Tel.: +96 47802840695; fax: +96 432327643.
E-mail address: abbasmatrood@yahoo.com (A.M. Bashi).

Peer review under responsibility of King Saud University.

Production and hosting by Elsevier

http://dx.doi.org/10.1016/j.arabjc.2012.03.015

Nanohybrid

anions are intercalated to give a biphasic well ordered nanohybrid material. The study of the release properties shows that both ions were released, but with different rates. This opens up the possibility of using such a biphasic nanohybrid for controlled release of more than one active anionic agent at different controlled rates.

1. Introduction

Layered double hydroxide (LDH), also called anionic clays, received considerable attention lately due to their potential applications in various areas of science and technology. LDHs are composed of brucite-like layers ($Mg(OH)_2$) containing M^{2+} and M^{3+} cations in an octahedral arrangement. Their general formula is $[M^{2+}_{1-x}(M^{3+}_{x}\ (OH)_2]^{x+}\ A^{n-}_{x/n}\cdot mH_2O$, where $M^{2+} = Mg^{2+}$, Ni^{2+}, Zn^{2+}, Cu^{2+}, Co^{2+}, etc., $M^{3+} = Al^{3+}$, Ga^{3+}, Fe^{3+}, Cr^{3+}, etc.; A^{n-} is an exchangeable anion, and the value of x ranges between 0.2 and 0.33. The partial replacement of M^{2+} by M^{3+} cation generates an excess of positive charge in the layers that is counterbalanced by anions located in the interlayer domains (Chao et al., 2000). A large variety of guest organic species in their anionic form such as drugs (Kwak et al., 2004), pesticides (Hu et al., 2007), dyes (Tian et al., 2007), can be incorporated into the interlayer space giving rise to host–guest hybrid materials useful for a controlled release formulation of 4-chlorophenoxy acetic acid as single molecular release from the layered double hydroxide (Hussein et al., 2007). The author shows the release of an individual anion(4CPA) intercalated with Zn/Al LDH; our work concerned two anions intercalated simultaneously. A wide range of applications has been particularly found in the field of health. Pharmaceutical products such as folic acid, fuchsin, antihypertensive and anti-inflammatory drugs have been thus intercalated (Hussein et al., 2005a; Wang et al., 2005b; Qin et al., 2008; Hussein et al., 2004) all of these references explained a single anion release. Host LDH is also useful as a nonviral vector (Ambrogi et al., 2001), or for DNA and ATP storage due to the high stability of these biological species in the interlamellae (Sasai et al., 1998). Another relevant application for the development of eco-friendly processes, concerns the adsorption and the controlled release of herbicides and pesticides (Malherbe et al., 1998; Cardoso and Valim, 2006).

Several methods are available to synthesize the organic molecules/LDH assemblies, i.e. co-precipitation, direct anionic exchange and reconstruction of the mixed oxide, which allow tuning of their properties and particularly controlled release (Pavlovic et al., 2005; Xu et al., 2006; Ledley, 1995; Kriven et al., 2004; Choy et al., 2000). The latter will indeed depend on the guest–host interactions, the local environment of the guest species, and the affinity of the incoming and outgoing anions. Moreover, parameters such as pH and composition of the host LDH are also crucial.

Previous works showed that 4-chlorophenoxy acetic acid (CPA) Hussein et al., 2007 and 2,4-dichlorophenoxy acetic acid (DPA) Hussein et al., 2005a can be intercalated into Zn-Al-LDH to give nanohybrids. The subsequent release of CPA and DPA were studied. However, in several cases a concurrent controlled release of these two herbicides is necessary. This was an incitement to study in this paper, the formation of a new biphasic organic–inorganic nanohybrid material by intercalation of both CPA and DPA guest entities into Zn-Al-LDH inorganic host. The co-precipitation method previously found highly efficient for the intercalation of the CPA or DPA species was preferably chosen. A study of the controlled release properties of the biphasic hybrids was also performed into an aqueous solution containing carbonate anions.

2. Materials and methods

2.1. *Synthesis of the Zn/Al LDH and the nanohybrids with DPA and/or CPA*

All chemicals used in the synthesis were obtained from various chemical suppliers and used without further purifications. All solutions were prepared using decarbonated and deionized water.

The formation of nanohybrids by intercalation into host Zn/Al LDH of DPA or CPA, on one hand, or of these two anions concurrently, on the other hand, was done by co-precipitation method. 50 ml of a single or mixed anions solution in ethanol (90%) of DPA (so many tests were done using different concentrations from the two guests molecules, the best results found experimentally were with the concentrations of 0.16 M and CPA (0.4 M)) and a mixed aqueous solution of $Zn(NO_3)_2{\cdot}6H_2O$ (0.1 M) and ($Al(NO_3)_3){\cdot}9H_2O$ (0.033 M), containing the required amounts having a Zn/Al molar ratio of 3, were precipitated maintaining pH at around 7.5. This was achieved by the slow addition of NaOH (2 M) under N_2 atmosphere with continuous vigorous stirring. The slurry obtained was aged for 18 h in an oil bath shaker at 70 °C. The resulting precipitate was centrifuged, washed 4 times with deionized water, and then dried in an oven at 70 °C overnight. Samples were kept in sample bottles for further use and characterizations. The hybrids intercalated with DPA, CPA and with both DPA and CPA were hereafter designated as DPA-Zn/Al, CPA-Zn/Al and DCPA-Zn/Al, respectively.

Similar procedure was used to prepare a Zn/Al LDH by co-precipitation of $Zn(NO_3)_2{\cdot}6H_2O$ (0.1 M) and $Al(NO_3)_3{\cdot}9H_2O$ (0.033 M) (Zn/Al = 3) with NaOH (2 M) at constant pH 7. Nitrates are the compensating anions of this Zn/Al LDH.

2.2. *Characterizations*

X-ray powder diffraction patterns (PXRD) were obtained with a Shimadzu XRD-6000 powder diffractometer using Cu Kα1 radiation ($\lambda = 1.540562$ Å) at 40 kV and 30 mA, scan rate = 0.5 min^{-1}.

Fourier transform infrared (FTIR) spectra were recorded using a Perkin–Elmer 1750X spectrophotometer on KBr pellets in the range of 4000–400 cm^{-1}. The elemental analysis of the samples was performed by inductively coupled plasma-atomic emission spectrophotometry (ICP-AES) using a Perkin–Elmer spectrophotometer Optima 2000DV under standard conditions. A CHNS-932(LECO) analyzer was used to determine the percentage of DPA and CPA. The TG/DTG experiments were carried out with a Setaram TG-DSC-11 apparatus with fully programmable heating and cooling sequence sweep gas valve switching and data analysis. N_2 sorption experiments at 77 K were carried out with a Micromeritics ASAP 2000 instrument. Specific surface areas were calculated using the BET method. Shimadzu GC–MS-QP5050Z with temperature program from 40–340 °C, column inlet pressure = 21 KPa, column flow 0.6 ml/min, linear velocity = 28.8 cm/s and split ratio = 14, for controlled release and a Parkin–Elmer spectrometer lambda 35 were used.

2.3. Release studies in aqueous solution

The release of the two phenoxyacetic acids of both DPA and CPA guest species, from the interlamellar domain of the biphasic DCPA nanohybrid was studied adding 0.6 mg of the as-prepared solid into 3.5 ml of a 5×10^{-4} M aqueous solution of sodium carbonate. The accumulated amount of species released into the solution was measured at regular intervals of time using UV–Visible Parkin–Elmer spectrophotometer lambda 35, at $\lambda_{\max} = 226.7$ and 229.4 nm for CPA and DPA, respectively. Carbonate anions act as the incoming exchangeable anion to replace the guests inside the inorganic Zn/Al LDH interlamellae.

3. Results and discussion

3.1. Structure and composition

PXRD of Zn/Al and of the three hybrid materials, i.e. DPA-Zn/Al, CPA-Zn/Al and DCPA-Zn/Al are shown in Fig. 1. All the materials show the characteristic PXRD patterns corresponding to LDH whose reflections can be indexed in a hexagonal lattice with R-3m rhombohedral symmetry. The (0 0 3) Bragg reflections for Zn/Al at 10.04 2Θ, corresponding to an interlayer distance of 0.88 nm, are in agreement with the presence of nitrates as compensating anions. The intercalation of the organic anions in the interlamellae of the host Zn/Al LDH is confirmed by the expansion of the d_{003} basal spacing to 1.97 and 2.54 nm for CPA-Zn/Al and DPA-Zn/Al, respectively. These values are in agreement with those previously reported (Hussein et al., 2007, 2005a). The intensity of the 00*l* peaks is rather similar in the host Zn/Al-LDH and the monophasic hybrids (DPA-Zn/Al and CPA-Zn/Al), therefore exhibiting closer crystallinities. Besides, a nanohybrid material with basal spacings of 2.54 and 1.99 nm was observed in the case of DCPA-Zn/Al. This shows that this biphasic nanohybrid is actually composed of 2 different types of interlamellae domains containing DPA and CPA anions, respectively. This may be due to the formation of a mixture of two phases which is thermodynamically more stable. Notably, for each phase, up to five (00*l*) harmonics are observed. Moreover, the crystallinity of DCPA-Zn/Al is greatly enhanced comparatively to the monophasic samples (CPA-Zn/Al and DPA-Zn/Al). These features account for the higher stacking order of the mixed biphasic nanocomposite. However, the formation of a small amount of mixed phases containing in the same interlamellae both DPA and CPA anions could not be totally ruled out, as will be discussed later in the direct insertion mass spectroscopy results.

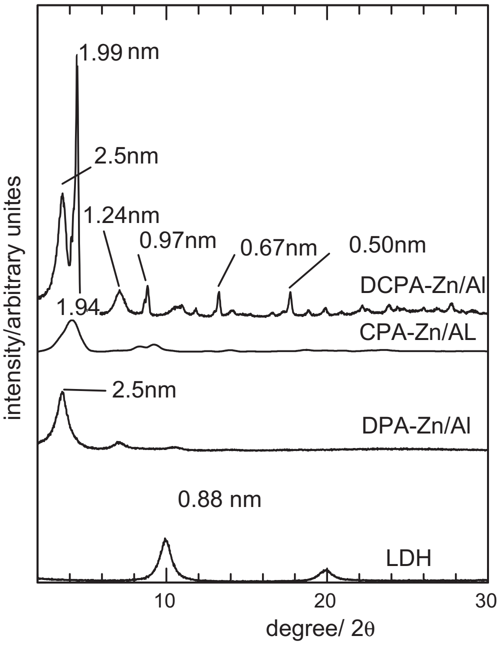

Figure 1 PXRD patterns of LDH, DPA, CPA, CDPA biphasic nanohybrid containing both 24D and 4CPA organic moieties synthesized at Zn to Al initial molar ratio, $R = 4$ (easy plot).

Elemental analysis of DCPA-Zn/Al leads to a Zn/Al molar ratio of 2.96, close to those of the precursors zinc and aluminum nitrate salts in the synthesis solution. The carbon content of about 22.4% confirms the intercalation of the carbon-containing guest molecules. However, this value is higher than that expected (~17 wt%) assuming a theoretical composition $[Zn_{0.75}\ Al_{0.25}(OH)_2]\ [DPA_{0.1875}\ CPA_{0.0625}]\cdot mH_2O$ for DCPA-Zn/Al if the initial NO_3^- of Zn/Al were exchanged by the DPA and CPA species with a molar ratio of CPA/DPA = 3 as in the synthesis solution. This suggests a CPA/DPA molar ratio larger than 3 in the nanohybrid.

Further physico-chemical characterizations and controlled release property will be then focused on the mixed biphasic nanohybrid that is more stable thermodynamically due to the originality of this material.

In order to confirm that DPA and CPA are actually both intercalated into the LDH interlamellae, DIMS analyses of DPA and CPA have been compared to that of DCPA-Zn/Al (Fig. 2). The main peaks observed correspond to m/z values of 128, 141, 186 in the case of CPA, and to m/z values of 162, 175, 220 in the case of DPA. Peaks corresponding to all previous m/z values are observed in DCPA-Zn/Al accounting for the presence of both anions in the interlamellar domain of the nanohybrid. It is worth noting the higher intensity of the peaks assigned to DPA than to CPA species, therefore suggesting higher intercalation rate of the former in agreement with the CPA/DPA molar ratio of 3 in the synthesis solution.

TGA/DTG profiles of Zn/Al and DCPA-Zn/Al nanohybrid are shown in Figs. 3a and b. Regarding Zn/Al the TG profile shows that the mass loss occurs in three different steps. The first step gives rise to a DTG peak at 109 °C and corresponds to a weight loss of 6.8% attributed to the removal of water molecules physically adsorbed on the layers surfaces (Kooli et al., 1997). The second step associated to a DTG peak at 239 °C and corresponding to a weight loss of 15.7%, is attributed to

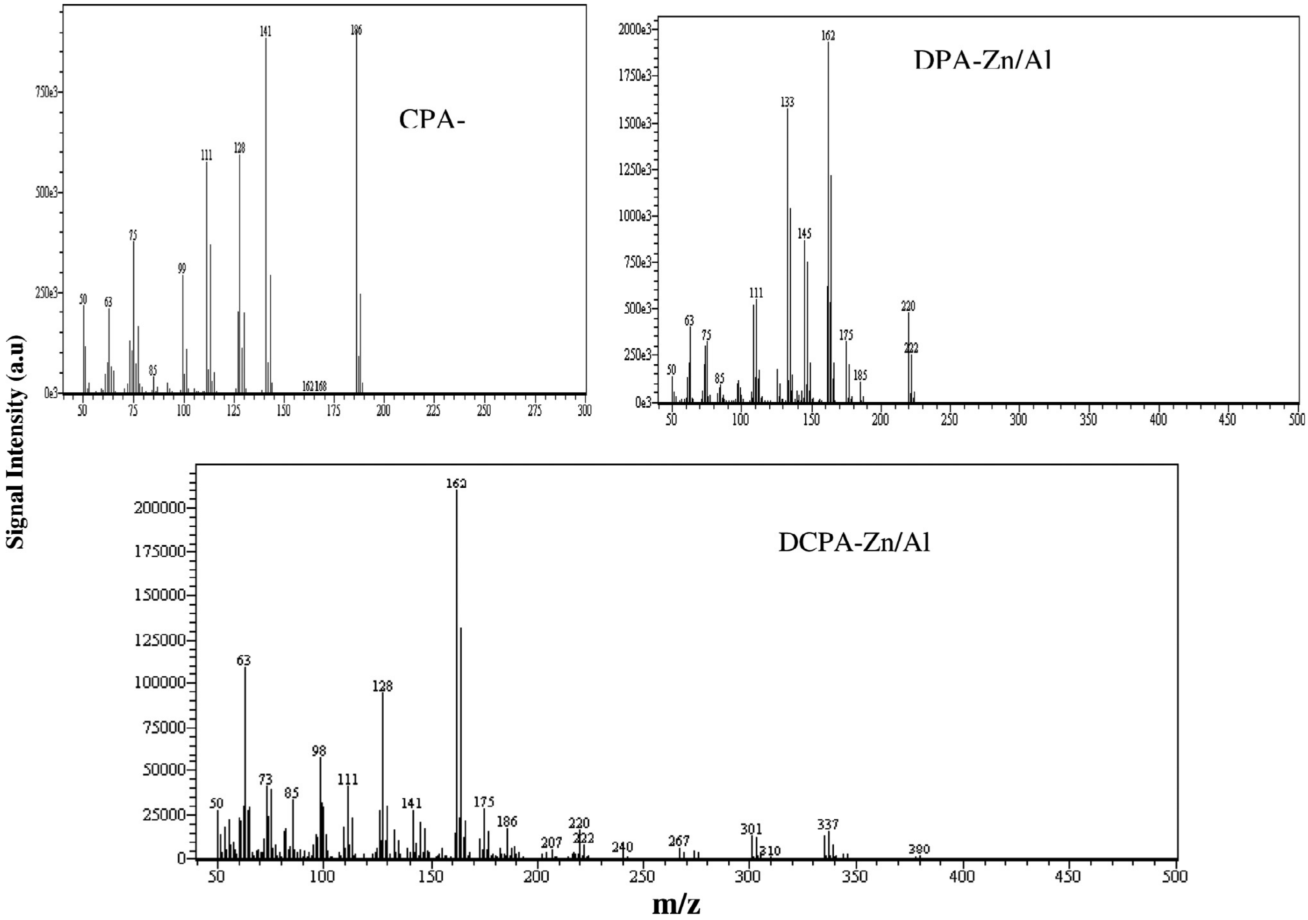

Figure 2 FIDMS of DPA-, CPA- and DCPA-Zn/Al phases shows the characteristic signal of DPA-Zn/Al and CPA-Zn/Al in the samples of DCPA-Zn/Al.

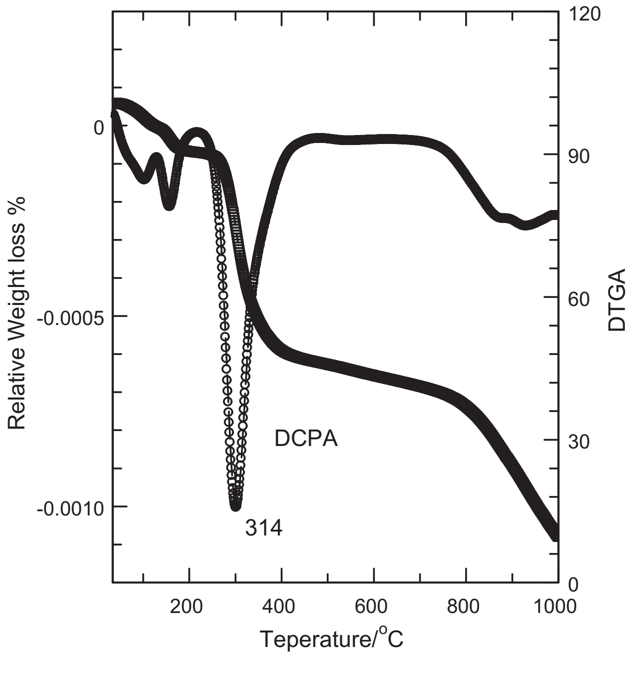

Figure 3a TGA/DTG thermograms of CDPA biphasic nanohybrid.

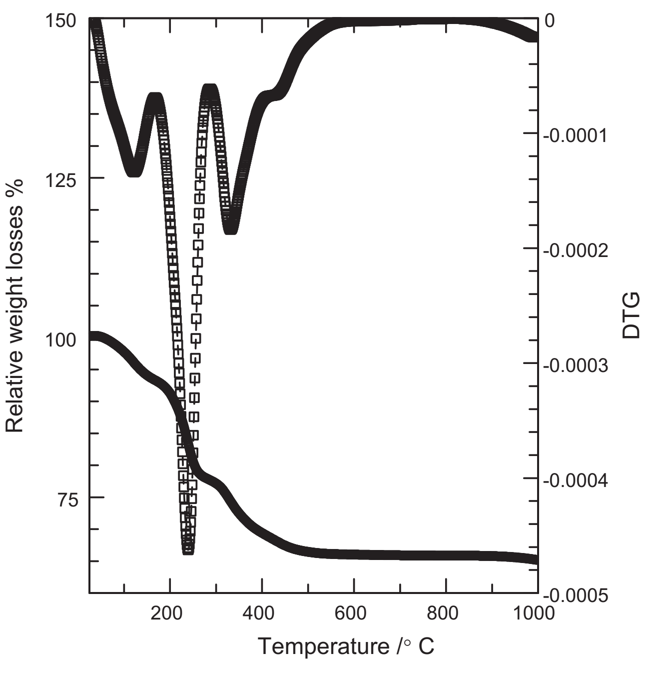

Figure 3b TGA/DTG thermograms of LDH.

the complete removal of the structural and interlayer water molecules. A third DTG peak at 330 °C, corresponding to a weight loss of 11.66%, can be assigned to the decomposition of the intercalated nitrate anions.

Three decomposition steps are also observed in the TG profile of DCPA-Zn/Al. However, they give rise to a very different DTG profile than Zn/Al. The first decomposition step is accompanied by two distinct DTG peaks in the region between 30–170 and 177–215 °C, with temperatures maximum at 122 and 166 °C, respectively. They are attributed to the removal of two different weakly bonded water molecules. The peak at 314 °C, can be assigned to the concurrent decomposition of the organic CPA and DPA anions, and the removal of water provided by the hydroxyl groups of the brucite-like sheets. Compared to Zn/Al, a new peak appears at 940 °C, which can be assigned to the removal of the last carbonaceous residues formed by the decomposition of the organic anions. These results concur with those reported earlier (Cavani et al., 1991).

Noteworthy, the total weight loss increases from 34% to 81% when going from Zn/Al to DCPA-Zn/Al. The former is in agreement with the expected value of 35.5%. The latter is also by far higher than that expected (~47.5%) assuming the theoretical composition $[Zn_{0.75}\ Al_{0.25}(OH)_2]\ [DCN_{0.1875}\ CPA_{0.0625}]\cdot mH_2O$ reported above. This shows that in addition to intercalation, large amounts of guest organic entities are probably adsorbed on the external surface of the sample.

The FTIR spectra of the host Zn/Al-LDH, the guest CPA, DPA species, and of the biphasic DCPA-Zn/Al nanohybrid are compared in Fig. 4. The broad band of O–H stretching at 3565 cm^{-1} in the Zn/Al-LDH is shifted to 3443 cm^{-1} in the DCPA-Zn/Al nanohybrid showing the different interactions with the brucite-like layers of the NO_3^- and the organic guest entities. Two bands at 1736 and 1412 cm^{-1} in DPA and CPA attributed to ν_{as} and ν_s vibrations of the carboxylate group of DPA and CPA are shifted to lower wave numbers, i.e. 1604 cm^{-1} in DCPA-Zn/Al confirming that the carboxyl groups are in a deprotonated form after intercalation. The bands at 1486 and 1421 cm^{-1} in DCPA-Zn/Al are attributed to the C=C vibrations of the aromatic rings, and those at 1334 and 1065 cm^{-1} to the ν_s and ν_{as} vibrations of the C–O–C bonds. The bands observed in the 2926–2917 cm^{-1} range are due to C–H stretching vibrations. A weak band at 1383 cm^{-1} in the spectra of DCPA-Zn/Al is due to a small amount of non exchanged NO_3^- of the Zn/Al host LDH, though not detected in the PXRD pattern of this nanohybrid (Fig. 1). The bands at 601 and 430 cm^{-1} are attributed to the Al-OH and Zn-Al-OH bending vibrations, respectively.

The nitrogen adsorption–desorption isotherms of DCPA-Zn/Al was done after pretreatment of degassing at 150 °C. This reveals a H3-type hysteresis loop in the IUPAC classification (Fig. 5a). There is no plateau at high P/P_0, therefore the adsorption isotherm cannot be regarded as Type IV. A Type IIb designation has been proposed for this isotherm given by aggregates of platy particles or adsorbents containing slit-shaped pores (Rouquerol et al., 1999). This behavior is in agreement with the lamellar structure of DCPA-Zn/Al. The specific surface area reaches 21 $m^2\ g^{-1}$. The pore size distribution was evaluated applying the B.J.H method to the desorption branch of the isotherm. There is a bimodal pore size distribution (Fig. 5b) with pores exhibiting average sizes at around 5 and 9.2 nm with a total pore volume of around 0.039 $cm^3\ g^{-1}$.

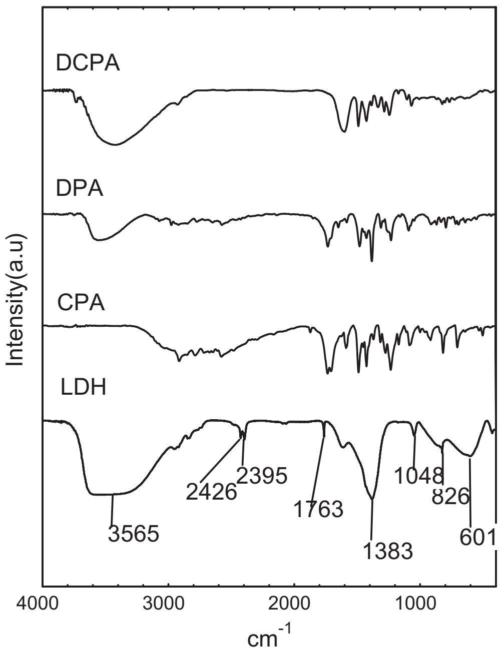

Figure 4 FTIR spectra of LDH, 24D, 4CPA and the biphasic nanohybrid, CDPA.

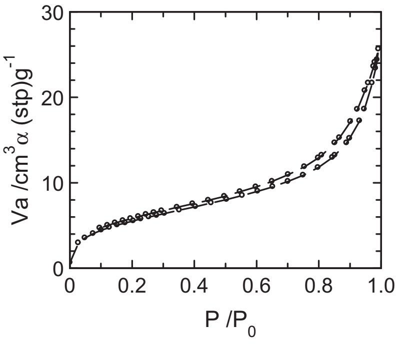

Figure 5a Type II adsorption–desorption isotherm of nitrogen gas at 77 K of biphasic nanohybrid.

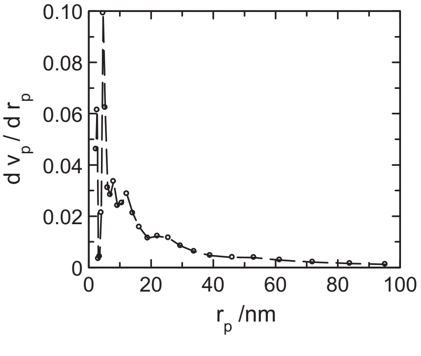

Figure 5b Morphology of LDH and the biphasic nanohybrid pore size distribution of biphasic nanohybrid.

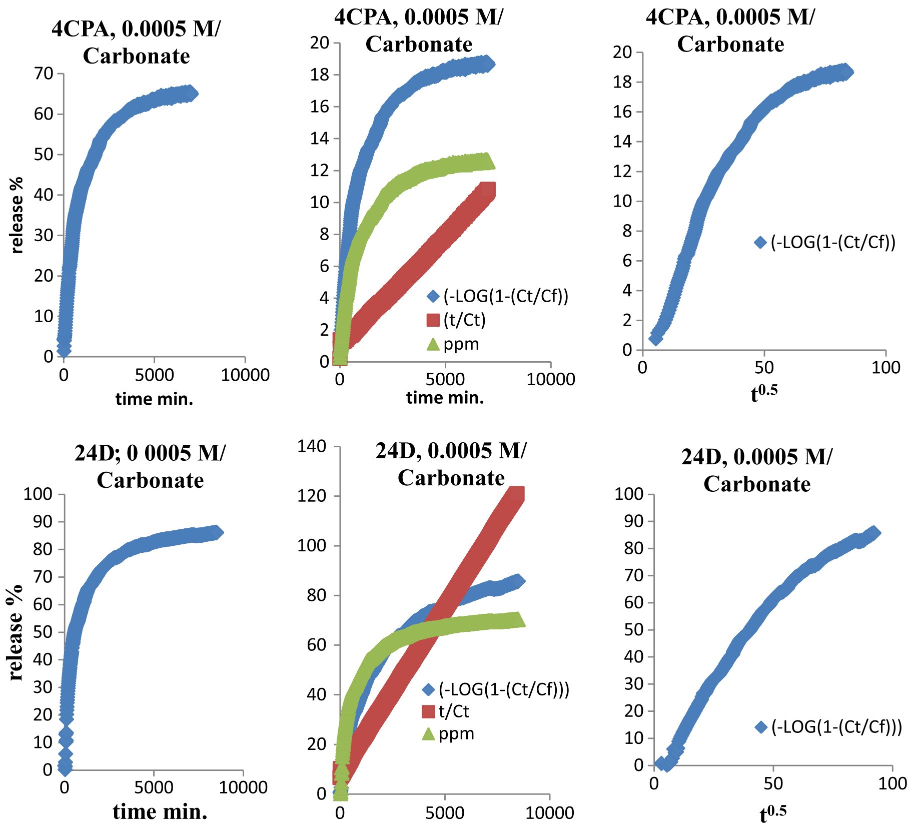

Figure 6 Fitting the data of simultaneous release of 4CPA from the DCPA-Zn/Al biphasic nanohybrid to zero order, first order, pseudo-second order and Bashker diffusion equation, C_i = initial concentration, C_f = final concentration, C_t = concentration at time (t), $x = C_i/C_{f.}$, t = time in minutes.

Table 1 Release of CPA and DPA into three different media of (Sodium Carbonate, Sodium Phosphate and Sodium Chloride) using three different concentrations.

Media	Conc.(M)	K (CPA)	r^2 (CPA)	K (2,4-D)	r^2 (2,4-D)
Na_2CO_3	0.500	0.000600	1.000	0.001610	1.000
	0.050	0.000600	1.000	0.001230	1.000
	0.005	0.000013	0.998	0.000060	1.000
Na_3PO_4	0.500	0.000060	0.951	0.000017	0.983
	0.050	0.000003	1.000	0.000017	0.999
	0.005	0.000025	0.994	0.000017	0.998
NaCl	0.500	0.000003	0.999	0.000013	0.999
	0.050	0.250000	0.998	0.000012	0.998
	0.005	0.000002	0.999	0.000011	0.999

3.2. 2. Controlled release of DPA and CPA

The release profiles of DPA and CPA from DCPA-Zn/Al into the aqueous solution of Na_2CO_3 (5×10^{-4} M) are given in Fig. 6. As a model of all the releases in different media both profiles have the same general shape with a faster release during 200 min and equilibrium achieved in 700 min. The rapid release suggests a large contribution of the ion exchange process with the carbonate anions. Indeed the affinity of carbonate for LDH is known to be very high. However DPA is released faster and leads to a higher accumulated amount than CPA, accumulated amounts released were 85.8 and 67% for DPA and CPA respectively measured by using the formula of Beer–Lambert law: A = a, b, c (where A is the absorbance, a is absorptivity, b is the light passage length in cm, c is concentration in ppm). Calibration curve was done for each anion only at fixed wavelength, using this calibration curve to calculate the amounts of anion released from the LDH to the different solutions medium, the following kinetic modules were attempted to fit the data obtained from the release of DPA and CPA species. For this purpose zero-, first-, pseudo-second order and parabolic diffusion equations ((1) – (4)) have been used:

(1) $C = kt$ (where C is the concentration in ppm, k rate constant and t is time in inutes.
(2) $-\log(1\text{-}C_t) = \log C_e - k\ t$ (C_t is initial concentration in ppm, k first order rate constant and t is time in minutes).
(3) $t/C_t = 1/k_2 \cdot C_e^2 + 1/C_e \cdot t$ (t is time in minutes, C_t is the concentrations at time t in ppm, C_e is the concentrations released at equilibrium).
(4) $C_t/C_{eq} = k \cdot t^{0.5}$ (C_t, C_{eq} are the concentrations in ppm at time t and at equilibrium time).

As shown in Fig. 6 and Table 1 the release of DPA and CPA in three media sodium carbonate, sodium phosphate and sodium chloride, follows with good accuracy the pseudo-second order model which gives the higher regression values.

The structure of the two molecules can account for their different release rates, the greater size of DPA than 4CPA factor is not considered but the electron acceptor ability of the two chlorides of DPA indeed decreases more the electron density localized on the carboxylate than one chloride of CPA, may be this is more significant for the easier release of the former species. The order of release according to the medium of incoming anions is $CO_3^{2-} > PO_4^{3-} > Cl^-$.

4. Conclusion

This study shows that the formation of a new biphasic nanohybrid containing two different anions, 2,4-dichlorophenoxy acetate and 4-chlorophenoxy acetate, can be accomplished by the direct co-precipitation method. The guest species are both intercalated into the Zn/Al-LDH thus giving a biphasic well ordered nanohybrid material. A controlled and simultaneous release of the two active agents can be performed, but at different rates. It is governed by a pseudo-second order kinetic. These results reveal the possibility of using biphasic nanohybrids for controlled release of more than one herbicide agent at the same time. This approach can probably find several applications in future with other types of herbicides that are able to give anionic species.

Acknowledgments

This work was funded by ITMA-UPM, Grant of research fellowship UPM/1.9.1. The authors thank ITMA-UPM for study leave and scholarship.

References

Ambrogi, V., Faredella, G., Gardolini, G., Perioli, L., 2001. J. Pharm. 220, 23.

Cardoso, L.P., Valim, J.B., 2006. J. Phys. Chem. Solid. 67, 987.

Cavani, F., Trifirb, F., Vaccari, A., 1991. Catal. Today 11 (2), 173.

Chao, Y., Chen, P., Wang, S.L., 2000. Appl. Clay Sci. 40, 193.

Choy, J., Kwak, S., Jeong, Y., Park, J., 2000. Angew. Chem., Int. Ed. 39, 4042.

Hu, Q., Xu, Z., Qiao, S., Haghseresh, F., Wilson, M., 2007. J. Colliod Interface Sci. 308, 291.

Hussein, A.H., Yahya, M., Shamsul, H.M., Salleh, T., Yap, J., Kin, J., 2004. Mater. Lett. 58 (3–4), 329.

Hussein, M.Z., Yahya, A.H., Zainal, Z., Kian, L.H., 2005a. J. Sci. Tech. Adv. Mater. 12 (6, 8), 956.

Hussein, M.Z., Sarijo, S.H., Yahya, A.H., Zainal, Z., 2007. Synth. J. Nano Sci. Tech. 7, 1.

Kooli, F., Depege, C., Ennaqadi, A., De Roy, A., Bess, J.P., 1997. Clay. Clay Miner. 45, 92.

Kriven, W.M., Kwak, S.Y., Wallig, M.A., Choy, J., 2004. MRS. Bull. 29, 33.

Kwak, S.Y., Kriven, W.M., Walling, M.A., Choy, J.H., 2004. Biometerials 25, 5995.

Ledley, F.D., 1995. Hum. Gene Therapy 6, 1129.

Malherbe, F., Forano, C., Sharma, B., Atkins, M.B., Besse, J.P., 1998. Appl. Clay Sci. 13 (5–6), 381.

Pavlovic, I., Barrigo, C., Hermosin, M.C., Corenjo, J., Ulibari, M.A., 2005. Appl. Clay Sci. 30, 125.

Qin, L., Wang, S., Zhang, R., Zhu, R., Sun, X., Yao, S., 2008. J. Phys. Chem. Solid. 69 (11), 2779.

Rouquerol, F., Rouquerol, J., Sing, K., 1999. In: Adsorption by Powders and Porous Solids. Principles. Methodology and Applications. Academic Press, London.

Sasai, R., Shinya, N., Shichi, T., Takagi, K., Gekko, K., 1998. Langmuir 15 (2), 413.

Tian, Y., Wang, G., Li, F., Evans, D.G., 2007. Mater. Lett. 61, 1662.

Wang, Z., Wang, E., GaO, L., 2005b. J. Sol. Stat. chem. 178 (3), 736.

Xu, Z.P., Zeng, Q.H., Lu, G.Q.M., Yu, A.B., 2006. Chem. Eng. Sci. 61, 1027–1040.